

PSInSAR Study of Lyngenfjord Norway, using TerraSAR – X Data

Udit Asopa^{1,*}, Shashi Kumar¹, Praveen Kumar Thakur¹

¹ Indian Institute of Remote Sensing, Dehradun, India – uditasopa.iirs@gmail.com, (shashi, praveen)@iirs.gov.in

Commission V, SS: Disaster Monitoring, Damage Assessment and Risk Reduction

KEY WORDS: PSInSAR, Permanent Scatterer, Lyngenfjord, Landslide, Subsidence

ABSTRACT:

In this research paper, focus is given on exploring the potential of Persistent Scatterer Interferometric Synthetic Aperture Radar (PSInSAR) technique for the measurement of landslide, which is the extension of existing DInSAR technique. In PSInSAR technique, the movement is measured by finding the phase shift in the scatterers present in the study area through the course of time. The backscattering of such a scatterer does not change during the study. By using this technique, 32 datasets acquired over a period of time i.e. from 2009 to 2011 over the area of Troms County of Lyngen Fjord, Norway are analysed. The dataset utilised are acquired with TerraSAR - X and TanDEM – X pair, in Stripmap mode of acquisition. Coregistration of dataset with subpixel accuracy is done with master images is done to align all the dataset correctly. APS estimation is done in order to remove the phase decorrelation caused by the atmosphere, movement, etc. using algorithms for phase unwrapping which allowed the processing of sparse data and the effect of atmosphere is reduced by doing analysis on temporal basis of the phase shift in interferograms of successive datasets. By this study it has been tried to show the estimation of shift can be done by the temporal analysis of the data acquired by TerraSAR X. The velocity output is displayed in a map reflecting the velocity of movement. Apart from this, the data properties such as baseline distribution both temporal and spatial are displayed in a chart. Other outputs obtained are the atmospheric Phase Screen, sparse point distribution, reflectivity map of the study area etc. are displayed using a map of terrain. The output velocity obtained of the terrain movement is found to be in the range of -40 mm/yr to -70 mm/yr.

1. INTRODUCTION

Persistent Scatterer or Permanent Scatterer Interferometry is a technique to study the displacement or movement in the terrain. Synthetic Aperture Radar has been used in many application. PSInSAR Technique is a derivation of DInSAR i.e. Differential Interferometric SAR technique, which is used in the study of change in the terrain feature. This method has been used in the monitoring of dams, excavations, while in research paper (Ge et al., 2001) it has introduced the use of DInSAR in glacier motion, volcanic activities, deformations due to earthquake, etc. For study the slope instability, InSAR data have been used in many researches such as in (Berardino et al., 2003; Lauknes et al., 2010). Although existing method DInSAR provides the deformation, a new method of finding the deformation with increased accuracy PSInSAR has also been used to find the deformation of many types of geographical feature which has been discussed in the research papers such as land feature subsidence monitoring in (Kim J. et al., 2007). The problem of atmospheric delay and decorrelation can be minimised using the technology of PSInSAR which gives the promising outcomes. The displacement maps with accuracy of millimetre level can be produced through this technique (Gonnuru et al., 2018). According to (Leijen, 2014) this technique is one of the time series approach and is based on the coherent phase history of point scatterers which means that the phase of these pixels is studied for some duration and the change in the phase is studied. To identify such pixels corresponding to the geographical features which are stable through the duration, many quantities such as Amplitude Stability Index (Amplitude Dispersion Index), Coherence, Spectral Phase Diversity, etc. can be calculated (Crosetto et al., 2016). For selecting such features whose reflectivity remains same (Permanent Scatterers) during the entire period of study, a set of images or dataset is required, which is acquired over a longer period of time as it can give us the correct estimate of deformation and its rate.

In calculating the deformation, the phase decorrelation caused by the content of atmosphere i.e. the presence of water vapour in atmosphere cause the delay in phase, creating a layer of phase which is termed as atmospheric phase screen (APS). To estimate the value of APS, the method of interpolation which is based on the stack creating mechanism and their connection using different graph style i.e. auto flower, Delaunay etc. is used.

Other than InSAR, methods for monitoring the surface are aerial photograph comparison as discussed in (Krainer et al., 2000), laser scanning and triangulation based ground survey as discussed in (Konrad et al., 1999), TLS in (Bauer et al., 2003), etc.

2. STUDY AREA

In this study PSInSAR method is applied to the subsidence in the Terrain due to landslide. This study has been done on the Lyngenfjord which is present in the Troms County in Norway which is displayed in figure 1. According to National Geographic Encyclopaedia “Fjords are a geological feature which are often set in U-Shaped valley with steep walls of rock on either side” (Society, 2018). The region of study is located at the North West aspect of Lyngenfjord in Troms County. The rockslides in this area are classified to high risk as the rocks or debris falling from the height of 600 m gain high speed and upon impact to sea surface, it can create big waves which can be the cause of major consequences such as tsunamis for nearby town which is disastrous for population living in that area and can affect nearby ecosystems. The study area has Caledonian Bedrock. As the study area is in Troms county of Norway and the rocks here dates back to 2.5 billion years also having the bedrock remnants of the 400-500 million years old Caledonian mountain range, which can be found alongside coast. In the study done by (Andresen, 2018) there are total of 133 unstable

* Corresponding author

rock slopes are present and detected in the Northern Norway. This study is focused onto one of these unstable rock slope which is shown in figure 2 using the reflectivity map made from the TerraSAR-X data. According to (H. overli Eriksen et al., 2017) This technique can be applied to the study of Rocks for the long term monitoring and found that the rocks are sliding down with velocity of 50 mm/yr.

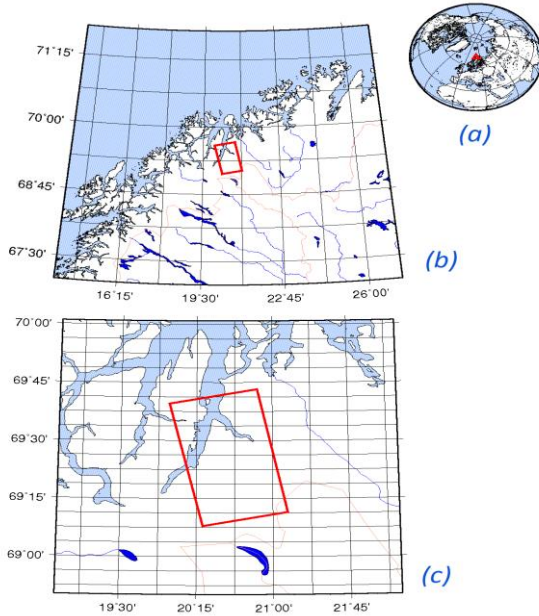


Figure 1 The Map of study area, (a) Global View, (b) Location of study area in Norway Country, (c) Enlarged View from (b)

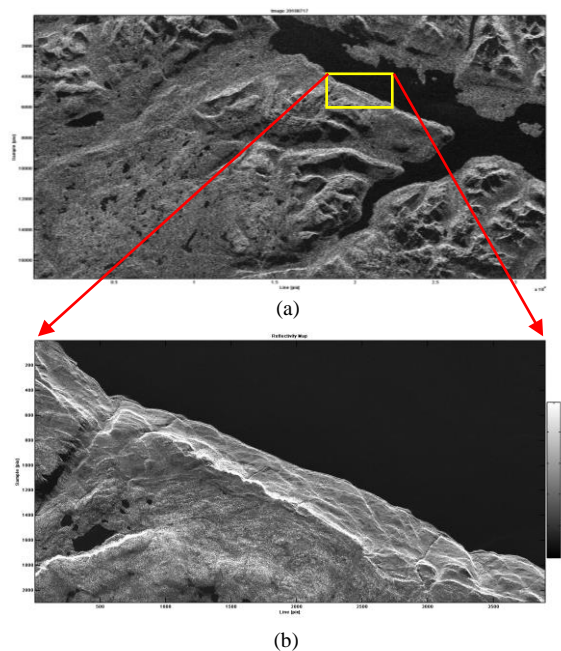


Figure 2 The reflectivity map (a) Complete Image (b) of Study Region

The geographical extent of dataset shown in image (a) covers area of 50 km x 30 km

3. DATASET

For this study the X band SAR dataset is used. These dataset are acquired by German Space Agency's Satellite TerraSAR - X and TanDEM – X. These two satellites feature a unique geometric accuracy that is unmatched by any other space borne sensor. The centre frequency of X band is 9.65 GHz. The dataset is acquired in Stripmap mode. In this mode of acquisition, a strip of ground area is illuminated continuously with fixed antenna beam in azimuth and elevation. Data acquired in this mode gives scene size of 30 km x 50 km on ground and with up to 3m spatial resolution. (Space, 2014)

The data used in this study is acquired in ascending pass of both satellites, having revisit time of 11 days. The datasets are acquired over a span of 836 days from 16 June 2009 to 30 Sept 2011. Table 1 shows the baseline distribution of datasets with respect to master image, where “Bn” is spatial baseline of datasets with respect to master dataset in meter and “Bt” is the temporal baseline of images with respect to the master in number of days. The baseline distribution table can easily be understood by looking at the graph in figure 3.

Table 1 Spatial & Temporal Baseline Distribution of dataset used with respect to the master image

Date of Acquisition	Polarization	Perpendicular Baseline (m)	Temporal Baseline (d)
20090616	VV	11	-396
20090627	VV	-39	-385
20090708	VV	-120	-374
20090719	VV	-23	-363
20090810	VV	23	-341
20090821	VV	-75	-330
20090901	VV	-4	-319
20090912	VV	180	-308
20090923	VV	160	-297
20091004	VV	5	-286
20091117	VV	-120	-242
20100523	VV	-70	-55
20100603	VV	-106	-44
20100614	VV	-184	-33
20100625	VV	-193	-22
20100706	VV	-42	-11
20100717	VV		Master Image
20100728	VV	-23	11
20100808	VV	-82	22
20100819	VV	0	33
20100830	VV	111	44
20100910	VV	10	55
20110601	VV	-147	319
20110623	VV	12	341
20110704	VV	-26	352
20110715	VV	-18	363
20110726	VV	-155	374
20110806	VV	-302	385
20110817	VV	-60	396
20110828	VV	-315	407
20110908	VV	0	418
20110930	VV	24	440

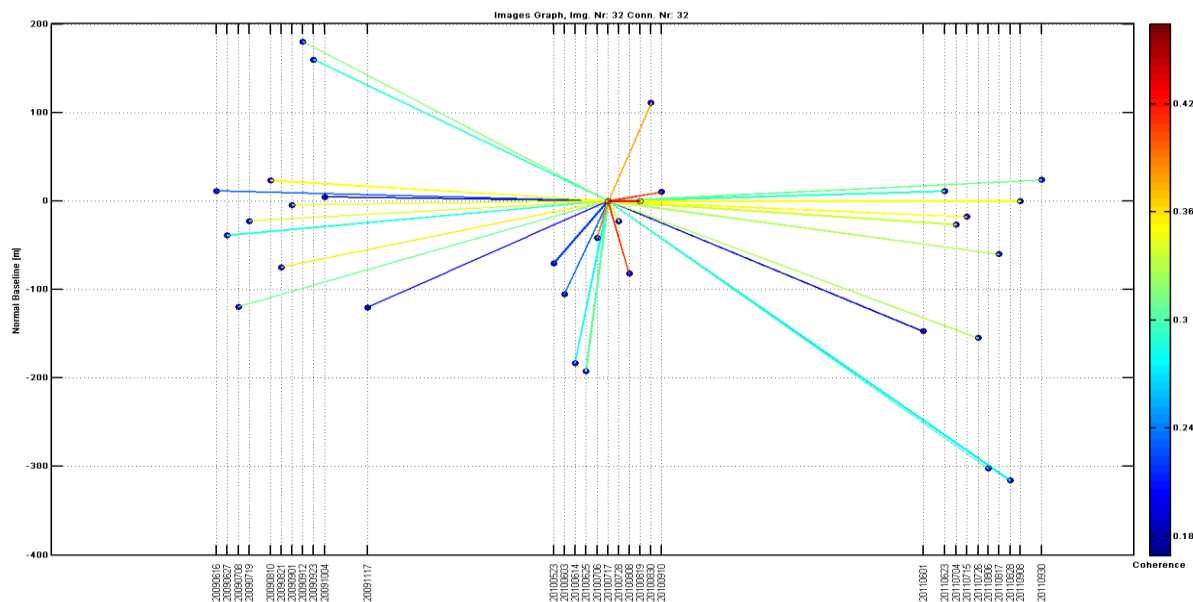


Figure 3 Baseline Distribution Graph of Dataset with coherence of each dataset with respect to Master Image

4. METHODOLOGY

The first step of processing the dataset is selecting the master image out of all, the master is selected by looking at the baseline distribution table of dataset. Master image should be selected in such a way that the baseline distribution becomes optimum. Here among all images, image acquired on 17 July, 2011 is selected as master image because it has optimum temporal and spatial baseline distance, giving maximum spatial baseline of slave images is 180 m and minimum is -315 m, temporal baseline maximum is 440 days and minimum is -396 days. Since the spatial area of each dataset is 30 km x 50 km, the area of master image which is common in all slave images is extracted out. For this study, maximum possible area is taken. The Coregistration is next step in which the pixels of slave images are matched and aligned according to the master image. Process of Coregistration is done with the subpixel accuracy. This is because Permanent scatterers are generally smaller in dimension than a ground pixel. Reflectivity map is important to be generated as it is generated over the co-registered datasets which are highly correlated to each other thus they have high value signal to noise ratio (SNR), which is important in study as it decrease the possibility of noise.

Some ground features are stable throughout the time and give high backscattering value, these features or scatterer are termed as permanent scatterers. There are many methods on selecting such scatterers, the method which is discussed and used in this study is amplitude stability index (ASI). In this method first amplitude stability index of whole scene is calculated then such cells which has high value of ASI than others are selected. The Amplitude Stability Index (ASI) is calculated using the value of Amplitude Dispersion Index (ADI). ADI for a particular pixel is calculated as given by eq. 1:

$$\sigma_A / \mu_A = D_A \quad \dots(1)$$

where

μ_A = mean

σ_A = standard deviation

D_A = Amplitude Dispersion Index

Thus amplitude stability index is calculated as given by eq. 2:

$$ASI = 1 - D_A = 1 - (\sigma_A / \mu_A) \quad \dots(2)$$

Amplitude Dispersion Index is the measure of the pixel's stability as high value of ADI means the less stability of pixel over time. For this study only those stable scatterers are taken into consideration which have value of ADI smaller than 0.15 i.e. the value of ASI is greater than 0.85. Such selected pixels have minimum decorrelation noise.

After generating the reflectivity map which gives us the grid output and makes selection of scatterers computationally fast. The grid insures the homogeneous distribution is sparse points. The topographic phase error is removed with the help of DEM employed, topographic phase error is the difference in height of scatterer obtained by the processing and the height of scatterer given by DEM. This product is also called residual topographic error. This process is called geocoding. Now up to this point grid of fine scatterers is obtained, out of which the persistent scatterer candidate (PSC) which have higher value than the threshold value of selecting criteria which is ASI in this study, are selected. As discussed earlier the ASI is set to 0.85 and there are 101 scatterers qualifying this criteria. This is done by loading the pixel matrix as mask from the reflectivity map grid (Perissin et al., 2007). These scatterers falls on a grid where the atmospheric component of noise is to be removed in order to eliminate the phase ambiguity. Atmospheric Phase Screen exhibits a low wave number spectral behaviour due to the presence of atmospheric water vapour thus introducing atmospheric phase errors. The process of its removal is done by creating a graph on selected image combination. For this study the Delaunay image combination is chosen for the processing. Delaunay image combination is made by interconnecting the datasets by connecting them using this triangulation method. By doing so, a network connecting all images is made and then cascaded LPF and HPF is applied on the image combination to estimate the decorrelation in spatial and temporal domain. These filters can also be applied on other image combination methods such as Auto Flowered (Centres or Clusters), Flowered, etc. Final output is generated after removing noises

and errors, which are atmospheric noise, flat earth error, displacement error and topographic error and phase noise. The above all steps are shown in the form of a flow chart in figure 4.

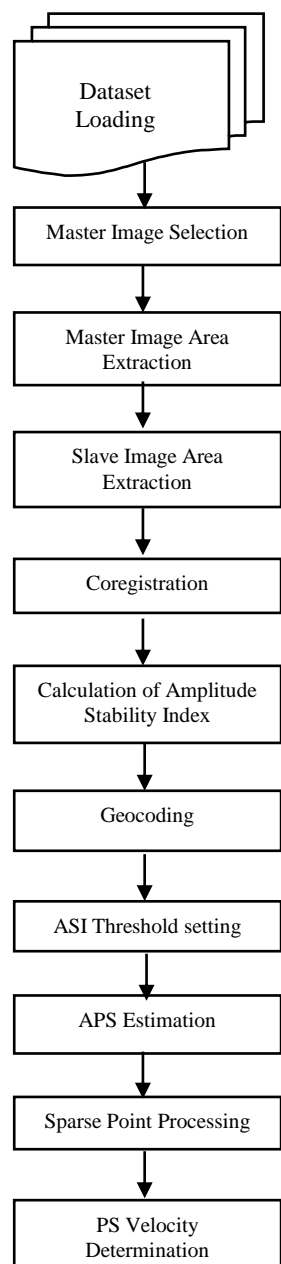


Figure 4 Methodology

Sparse points are eligible pixels to become a persistent scatterer. After estimating the phase errors and reference point, coherence and other parameters are calculated based on those estimated values. Finally the plot is generated by selecting those points which fill the criteria of having certain temporal stability, reflectivity & deformation trend. Such scatter points are plotted according to their geographic location on the reflectivity map to represent the location of velocity of terrain feature.

5. RESULT & DISCUSSION

The graph of baseline distribution of datasets drawn between baseline distance and time is displayed in figure 3 along with the coherence of each image with respect to master image. The coherency of these images means the phase difference between them, higher the coherency, lower the phase difference. Reflectivity map of region of study is shown in figure 5, the range of reflectivity is 0 to 3. After the generation of reflectivity map, Amplitude Stability Index for whole image is calculated. From ASI of whole image, only those pixels are taken for study which cross the threshold of having value of ASI greater than 0.85. These are the ground feature which shifted with time. All these pixels are represented in figure 6.

Atmospheric Phase Screen i.e. APS has been observed to be varying with every image. The phase ranges between $-\pi$ to $+\pi$ in APS of every image. APS on image acquired on 28 July, 2010 which has temporal baseline of 11 days with respect to master, is found to be varying between the same ranges. The estimated APS for image acquired on 28 July, 2010 is displayed in figure 7. After generation and estimating the APS for every dataset, the APS effect is applied to the image combination and the sparse points are processed to estimate the deformation. The range and criteria on which the selection of PS points is done, are set. Criteria such as Linear Trend and Height are set. The range of linear trend is set between -100 and +100, the range of Height is set to -100 to +100.

Finally the output result of deformation trend is calculated, which is generated between -100 to +100. Other criteria which are used to generate the suitable output such as reflectivity, deformation trend ranging between -100 and 0. The negative range of deformation trend is because the study region having the displacement in the direction away from the satellite sensor i.e. the elevation is decreasing. This negative displacement is due to the landslide in that area. The displacement is displayed in the figure 8. The number of sparse points crossing the threshold are 94 i.e. there are only 94 sparse points that represent the displacement in the study region. The output of this study is found to be in approximately -60 mm/year. The output is displayed in figure 8.

The Reflectivity map displayed in figure 5 is generated by taking mean of intensity of every dataset taken for study. The range of reflectivity map is between 0 – 3, here 0 represents the darkest pixel and 3 represents the brightest pixel. From the reflectivity map it can be clearly seen that in the region of study there are many pixels having high reflectivity which means that the backscatter from that particular ground resolution cell is stable through time, as an example the patch of dark pixel is represents the presence of water body there and no persistent scatterer candidate is present in that region. All these permanent scatterer candidate have the value of amplitude stability index higher than 0.85. The yellow circle in the reflectivity map shown in figure 5 displays the region of study. In this region of study the sparse points found are shown in black circle in the figure 6. From the figure it is visible that the no. of scatterers present in the region of study are very high as from the reflectivity map it is very clear that the reflection of pixels in this region (circled) is very high thus qualifying the pixels to be PSC. The graph method for estimate the APS requires the grid position of PSC. After making the grid, APS is estimated by making the centred flower connection between the sparse points.

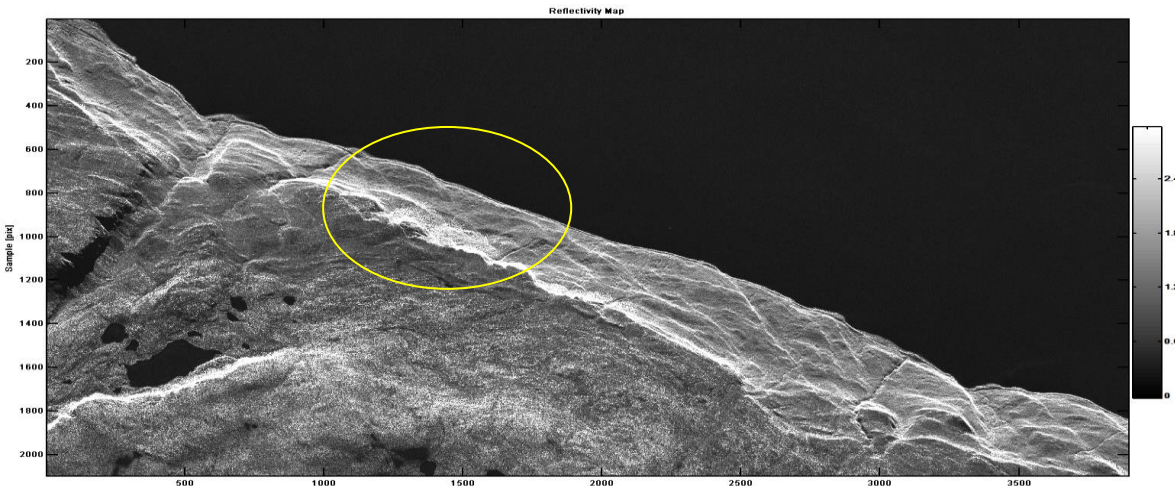


Figure 5 Reflectivity Map of the Region of Study

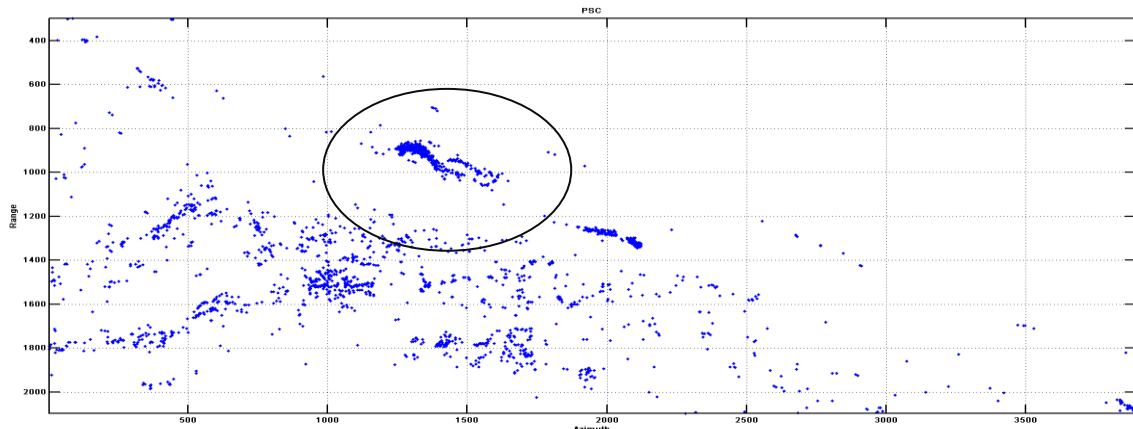


Figure 6 Permanent Scatters Candidate recognised in the Study Area

The estimated APS which is represented in figure 7 shows APS from 4 images taken from dataset. These APS are of dates 10th August 2009, 6th July 2010, 28th July 2010 and 6th August 2011. Out of these four images, APS of 6th July 2010 and 28th July 2010 are of before and after the Master Image. All APS are calculated with respect to Master Image. The study region is having variation in phase across time. In the displayed APS images, the black circle shows the study region. These changes occurring in the phase is due to the change in atmosphere over the area. The change in the atmospheric conditions can change the phase because of the change in the rate of humidity or water vapour present over that area.

The Displacement map is displayed in the figure 8 which is derived from the study of these datasets. The displacement displayed in the figure gives us the output of subsidence occurred in the north-western aspect of the study area in the west direction. The rate of shift is higher in the low elevated area and lower in the high elevated area. According to the geology of the study area, the slope is highly steep & these rocks have fractures, cracks, scraps and numerous ridges and gullies thus due to the bedrock foliation there is a good chance of sliding in the region. According to (Wang et al., 2015) melting of snow can also be the reason of landslide.

If the GNSS stations is applied on this area, there can be some more results like 3D displacement vector can be made and a Rock Slope Failure Model can be made which can help the government in preventing the loss to life and property in towns which are in vicinity. The loss to the ecosystem needs to be

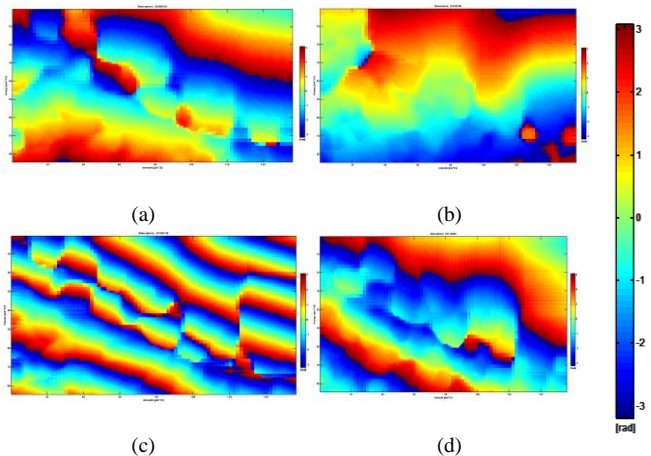


Figure 7 Estimated APS on (a) 10 Aug, 2009 (b) 6 July, 2010
 (c) 28 July, 2010 (d) 6 Aug, 2011

minimised in the occurrence of such event. Along with GNSS data acquisition setting, if geological survey is also done then the study of landslide can be done along with the idea about possibility of landslide due to the fractures and other geological setting of the area. If Instead of space borne TerraSAR-X data, airborne or ground based data is taken then the results obtained could be refined as the temporal difference in two consecutive datasets is at least 11 days while air borne or ground based have smaller temporal difference in between them.(Eriksen, Bergh, et al., 2017)

This contribution has been peer-reviewed. The double-blind peer-review was conducted on the basis of the full paper.

<https://doi.org/10.5194/isprs-annals-IV-5-245-2018> | © Authors 2018. CC BY 4.0 License.

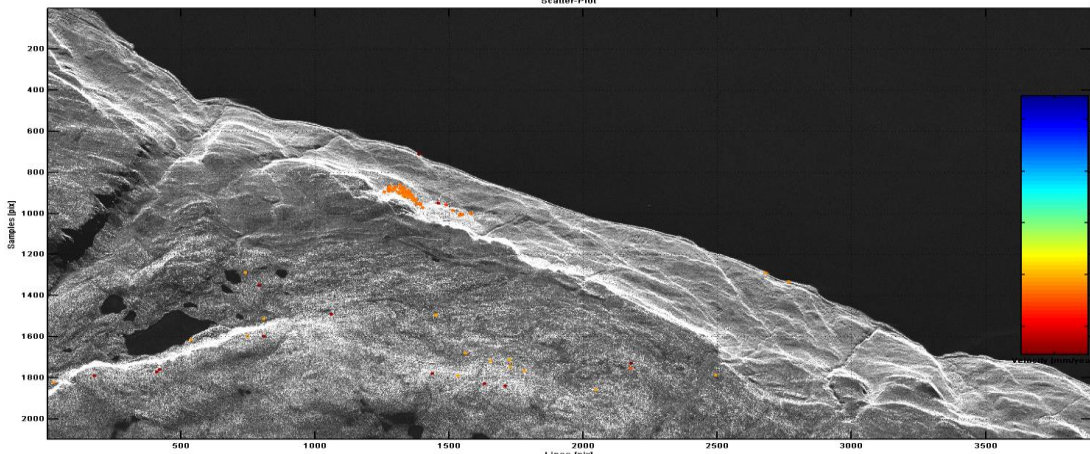


Figure. 8 Subsidence map obtained through the PSInSAR Processing of study area

6. CONCLUSION

The Study carried on the Lyngenfjord region of Norway using the PSInSAR technique of SAR, has given us the output subsidence rate of 60 mm/yr. This rate of subsidence means is proof of landslide occurred in that area. The Technique PSInSAR outputs results with very high accuracy. As the study was done to find the potential of PSInSAR technique, in overcoming the decorrelation noise introduced due to the atmosphere and other factors. Total of 32 images or datasets acquired over the period of 8 were used to infer the results. These datasets were used to generate the reflectivity map, interferometric phase difference, etc. The coherency of datasets were proven by the step of Coregistration. The output deformation trend is found to be - 60 mm/year which is near to the result obtained in the study (Eriksen, Bergh, et al., 2017). In this study authors found the deformation trend in the study region and cross referenced with the help of ground survey. Thus the output obtained in this case study is found to be matching with the already done research. That's how it can be said that the PSInSAR study is capable of finding the deformation trend with high accuracy. The Dataset obtained by TerraSAR-X are suitable for Coregistration as they are coherent to each other. From the study done for this project, the results suggest that there is high risk for nearby towns and community as there are highly unstable rockslide can possibly create tsunami as debris falling from the height of 400-500 m are very lethal and can give rise to the high waves that can travel up to 5 km and can hit town. So, the government can take safety measures from such studies and prevent the loss of life and property.

7. FUTURE RESEARCH SCOPE

The future extension of this study can be carried out by combining the methods of PSInSAR study and Tomography, from which the 4D Reconstruction of features can be done, which might help in the restoration of archaeological sites, to obtain the change in biophysical parameters of forest.

8. ACKNOWLEDGEMENT

The authors are very grateful to German Space Agency (DLR) for providing the Data of TerraSAR-X and TanDEM-X for study and research purpose. The Software used in this study is SARPROZ (SAR PROcessing software by Perrissin), for which authors show their sincere regard and thank SARPROZ Team for providing the evaluation licence of software. To carry out this case study, the Department of Photogrammetry and Remote Sensing, IIRS, India has provided the lab facility and for this, authors are grateful.

9. REFERENCES

- Andresen, M. L. (2018). *Regional structural analysis of rock slope failure types, mechanisms and controlling bedrock structures in Kåfjorden, Troms*. UiT The Arctic University of Norway. Retrieved from <http://hdl.handle.net/10037/12887>
- Bauer, A., Paar, G., & Kaufmann, V. (2003). Terrestrial laser scanning for rock glacier monitoring. In M. Phillips, S. M. Springman, & L. U. Arenson (Eds.), *Proceedings of the 8th International Conference on Permafrost, Zurich* (Vol. 1, pp. 55–60). Zurich: A.A. Balkema. Retrieved from http://research.iarc.uaf.edu/NICOP/DVD/ICOP_Permafrost/Pdf/Chapter_011.pdf
- Berardino, P., Costantini, M., Franceschetti, G., Iodice, A., Pietranera, L., & Rizzo, V. (2003). Use of differential SAR interferometry in monitoring and modelling large slope instability at Maratea (Basilicata, Italy). *Engineering Geology*, 68(1–2), 31–51. [https://doi.org/10.1016/S0013-7952\(02\)00197-7](https://doi.org/10.1016/S0013-7952(02)00197-7)
- Crosetto, M., Monserrat, O., Cuevas-González, M., Devanthéry, N., & Crippa, B. (2016). Persistent Scatterer Interferometry: A review. *ISPRS Journal of Photogrammetry and Remote Sensing*, 115, 78–89. <https://doi.org/10.1016/j.isprsjprs.2015.10.011>
- Eriksen, H. Ø., Lauknes, T. R., Larsen, Y., Corner, G. D., Bergh, S. G., Dehls, J., & Kierulf, H. P. (2017). Visualizing and interpreting surface displacement patterns on unstable slopes using multi-geometry satellite SAR interferometry (2D InSAR). *Remote Sensing of Environment*, 191, 297–312. <https://doi.org/10.1016/j.rse.2016.12.024>
- Eriksen, H. Ø., Bergh, S. G., Larsen, Y., Skrede, I., Kristensen, L., Lauknes, T. R., ... Kierulf, H. P. (2017). Relating 3D surface displacement from satellite- and ground-based InSAR to structures and geomorphology of the Jettan rockslide, northern Norway. *Norwegian Journal of Geology*, 97(4), 233–253. <https://doi.org/https://dx.doi.org/10.17850/njg97-4-03>
- Ge, L., Chang, H., & Rizos, C. (2004). Satellite radar interferometry for mine subsidence monitoring. <https://www.researchgate.net/publication/228847412>
- Gonnuru, P., & Kumar, S. (2018). PsInSAR based land subsidence estimation of Burgan oil field using TerraSAR-X data. *Remote Sensing Applications: Society and Environment* (Vol. 9). Elsevier B.V. <https://doi.org/10.1016/j.rsase.2017.11.003>

Konrad, S. K., Humphrey, N. F., Steig, E. J., Clark, D. H., Jr, N. P., & Pfeffer, W. T. (1999). Rock glacier dynamics and paleoclimatic implications. *Geology*, 27(12), 1131–1134. [https://doi.org/10.1130/0091-7613\(1999\)027<1131:RGDAP>2.3.CO;2](https://doi.org/10.1130/0091-7613(1999)027<1131:RGDAP>2.3.CO;2)

Krainer, K., & Mostler, W. (2000). Reichenkar rock glacier: A glacier derived debris-ice system in the western Stubai Alps, Austria. *Permafrost and Periglacial Processes*, 11(3), 267–275. [https://doi.org/10.1002/1099-1530\(200007/09\)11:3<267::AID-PPP350>3.0.CO;2-E](https://doi.org/10.1002/1099-1530(200007/09)11:3<267::AID-PPP350>3.0.CO;2-E)

Lauknes, T. R., Shanker, A. P., Dehls, J. F., Zebker, H. A., Henderson, I. H. C., & Larsen, Y. (2010). Detailed rockslide mapping in northern Norway with small baseline and persistent scatterer interferometric SAR time series methods. *Remote Sensing of Environment*, 114(9), 2097–2109. <https://doi.org/10.1016/j.rse.2010.04.015>

Leijen, F. van. (2014). *Persistent Scatterer Interferometry based on geodetic estimation theory*. Delft University of Technology. <https://doi.org/10.4233/uuid:5dba48d7-ee26-4449-b674-caa8df93e71e>

Perissin, D., & Ferretti, A. (2007). Urban-target recognition by means of repeated spaceborne SAR images. *IEEE Transactions on Geoscience and Remote Sensing*, 45(12), 4043–4058. <https://doi.org/10.1109/TGRS.2007.906092>

Society, N. G. (2018). Fjord - National Geographic Society. Retrieved July 30, 2018, from <https://www.nationalgeographic.org/encyclopedia/fjord/>

Space, A. D. and. (2014). TerraSAR-X Services Image Product Guide. *Technical Document*. Airbus Defence and Space. Retrieved from http://www2.geo-airbusds.com/files/pmedia/public/r459_9_201408_tsxx-itd-ma-0009_tsx-productguide_i2.00.pdf

Wang, Z. Y., Lee, J. H. W., & Melching, C. S. (2015). Debris Flows and Landslides. In *River Dynamics and Integrated River Management* (pp. 193–264). Berlin, Heidelberg: Springer Berlin Heidelberg. https://doi.org/10.1007/978-3-642-25652-3_5